Can added-mass variation act as a thrust force?

Francesco Giorgio-Serchi
Fluid Structure Interaction
Engineering and the Environment
University of Southampton
Southampton, UK
Email: f.giorgio-serchi@soton.ac.uk

Gabriel D. Weymouth
Fluid Structure Interaction
Engineering and the Environment
University of Southampton
Southampton, UK
Email: g.d.weymouth@soton.ac.uk

***Abstract*—Previous studies have demonstrated that added-mass variation can play a significant role on thrust generation. In this respect, a simplified mechanical system such as an aquatic shape-changing linear oscillator lends itself to this study because it allows to segregate the contribution of added-mass variation from other terms. We present the design of an experimental apparatus which highlights the capability of a deformable oscillator to drive sustained resonance by exploiting the thrust produced by shape-change alone. These results will have significant implications in aquatic propulsion and in the design of deformable, self-propelled underwater vehicles.**

I. Introduction

Recent studies on waterborne bodies subject to abrupt shape-change show that the associated added-mass variation can significantly participate in the generation of thrust, [1], [2]. This phenomenon is distinctive of the locomotion strategy of certain aquatic organisms such as octopi and squids, [3]. These organisms propel themselves by performing discontinuous expulsion of water jets via a routine of inflation and deflation of an elastic chamber. While the interest towards pulsed-jet propulsion has been mainly centred around the nature of the expelled vortex [4], lately the contribution to thrust from the external shape variation has earned recognition, [5].

The capability to exploit added-mass variation as a potential source of thrust has significant implications in the design [6] and modelling [7], [8] of new kinds of underwater vehicles. To study this phenomenon experimentally we focus on a simple mechanical apparatus, i.e. a submerged harmonic oscillator, where the role of shape-variation on the dynamics of the system can be segregated from other terms.

II. Added-mass as a source of thrust

An harmonic oscillator immersed in a dense, viscous fluid is described by the Morison force [9]. In the case of a 1 dof oscillator such as that schematically depicted in Fig. 1, the dynamics reads:

$$\frac{d}{dt}\left(m^*\dot{x}\right) = -\frac{1}{2}\rho_f C_d A \dot{x}|\dot{x}| + kx \tag{1}$$

where the effective mass is $m^* = m + m_a$, with m and m_a being the actual and added-mass, while $x(t)$ and k define the position and the elastic constant of the oscillator. In eq. (1) the differential sign in front of the inertial term is retained in order to account for added-mass variation effects.

In the assumption where the mass of the body varies negligibly, $\dot{m} = 0$, while its shape, and hence its added-mass, is altered, $\dot{m}_a \neq 0$, differentiation of eq. (1) yields,

$$\left(m + m_a\right)\ddot{x} = -\frac{1}{2}\rho_f C_d A \dot{x}|\dot{x}| + kx - \dot{m}_a\dot{x}. \tag{2}$$

Here, $m_a(t)$, represents the time-dependent added-mass, while $\dot{m}_a\dot{x}$ is the added-mass variation whose form is resemblant of a thrust term.

In the case of an harmonic oscillator, the fact that added-mass variation may act as a propelling force can be tested by rearranging eq. (2) such that:

$$\left(m + m_a\right)\ddot{x} = -\left(\frac{1}{2}\rho_f C_d A|\dot{x}| - \dot{m}_a\right)\dot{x} + kx. \tag{3}$$

which proves that a function of $\dot{m}_a$ must exist based on which the viscous term can be annihilated, i.e.

$$\dot{m}_a = \frac{1}{2}\rho_f C_d A|\dot{x}| \tag{4}$$

When the condition prescribed in eq. (4) is verified, the oscillator is driven into resonance, effectively behaving like an undamped system.

III. Shape-changing oscillator

In order to validate the hypothesis postulated in section II, we devise an experimental apparatus capable of replicating the dynamics described in eq. (3) based on the shape-changing routine of eq. (4). While the result reported in eq. (4) stands valid regardless of the shape of the oscillator, experimental

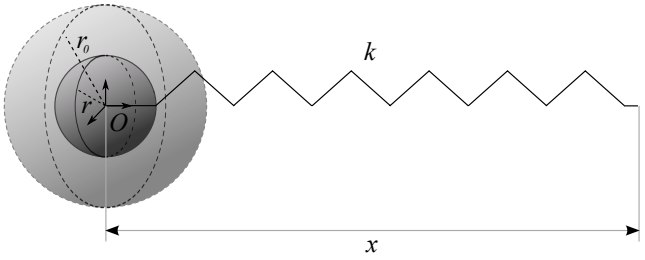

Fig. 1. Scheme of the shape-changing spring-mass oscillator. Here r represents the radius of the oscillator at time t, while r_0 refers to the mean radius of the oscillator. The distance of the frame of reference centred in O from the relaxation point of the spring is x. Taken from [10] with permission of Springer.

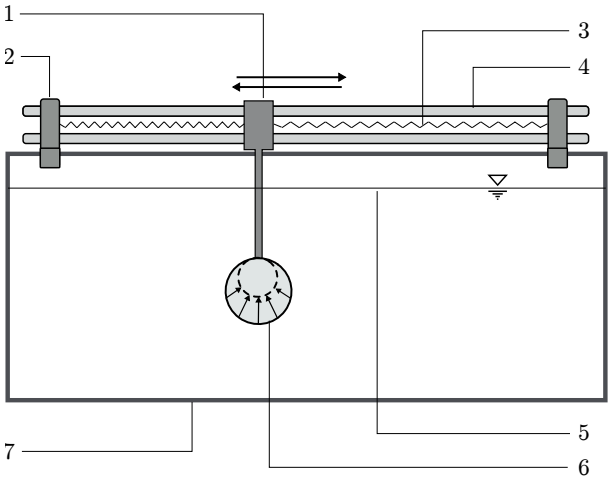

Fig. 2. Design of the experimental apparatus for testing the shape-changing harmonic oscillator: (1) slider unit with coupled frictionless bushings, (2) shaft support with spring mounts, (3) tension springs, (4) cylindrical shafts, (5) water level at free surface, (6) shape-changing spherical bob, (7) plexiglass tank.

verification of such formulation requires adequate simplification. To do so, we focus our experiments on a spherical body oscillating horizontally in water.

The experimental apparatus, Fig. 2, consists of two frictionless linear bushings sliding along two cylindrical shafts. The slider system is fitted above a tank filled with water. The tank is 200.0 cm long, 100.0 cm wide and 80.0 cm deep. The slider also mounts a slender cylindrical rod, the bottom end of which is immersed in water. A hollow spherical bob composed of rubber-like material is sealed to the cylindrical rod and is kept pre-stretched by inflating it with air. The air supply is provided via the cylindrical rod, which is hollow and allows to be fitted with an external oscillating pump. The actuation of the pump is responsible for regulating the shape-changing routine of the elastic spherical bob. The oscillatory behaviour of the system is granted by tension springs which connect the slider to a series of fixed points at the end walls of the tank.

By inflating the spherical bob with air the conditions which we have employed to derive eq. (2), where the oscillator varies its own added-mass while maintaining its inertia negligible, is verified. In addition, thanks to this design the forces along the vertical direction due to buoyancy and those in the horizontal direction remain fully decoupled.

In the case of a spherical bob, the shape-change routine capable of cancelling viscous drag can be determined by simply recalling that

$$m_a = \frac{2}{3}\rho_f \pi r^3, \tag{5}$$

with $r(t)$ being the time-dependent radius of the sphere, and hence

$$\dot{m}_a = 2\pi\rho_f r^2 \dot{r} \tag{6}$$

Thus, substitution of eq.(6) into eq.(4) shows that the condition for drag cancellation is met when,

$$\dot{r} = -\frac{1}{4} C_d |\dot{x}|. \tag{7}$$

As in standard parametric oscillators, [11], persistent resonance occurs as long as the routine of shape change is performed at twice the natural frequency $\omega_n = \sqrt{\frac{k}{m^*}}$.

The inflation/deflation routine prescribed by eq. (7) requires the spherical bob of the oscillator to shrink as long as the body is in motion and then abruptly inflate as it reaches the end of the stroke, i.e. when its velocity is instantaneously zero. This routine has been studied numerically in [5] with a fully coupled fluid-solid interaction solver. However, more smoothly varying shape-change routine would better suite experimental analysis. To this end it can be shown, [5], that any inflation/deflation routine capable of zeroing the power loss due to fluid forces will suffice to drive the oscillator into resonance. Hence we will employ a prescribed routine of the form:

$$r(t) = r_0 + a\sin(2\omega_n t) \tag{8}$$

with r_0 being the mean radius and $a > 0.1$ the coefficient of shape-change amplitude.

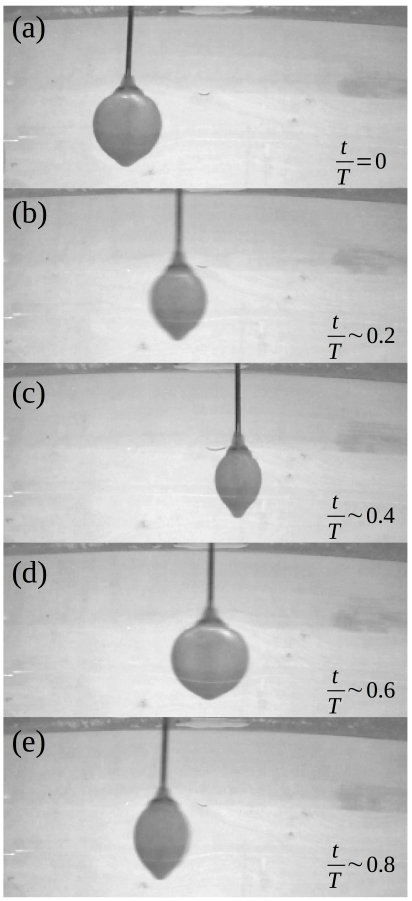

Fig. 3. The routine of shape change during one oscillation.

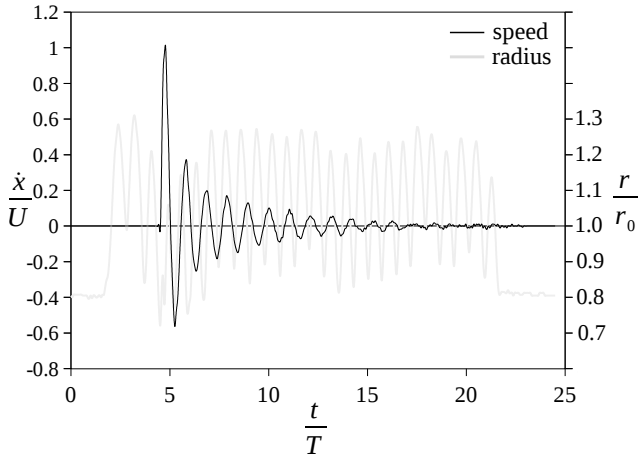

Fig. 4. Radius change profile and translational velocity (with U being the maximum velocity measured) of the oscillator in the case of $\omega_n = 2.0$ Hz.

IV. Experimental analysis

The experiments consist in displacing the spherical bob from its equilibrium position, thus pre-tensioning the springs, inflating the bob to the desired radius and then abruptly releasing it. The bob oscillates in water like a typical non-linearly damped spring-damper system. The displacement of the bob and its radius-change routine are recorded via an image-tracking system. We performed tests at two different natural frequencies $\omega_n \sim 1.0$ Hz and $\omega_n \sim 2.0$ Hz, the former of which is achieved by increasing m. For each of these we test three shape configurations: a fixed-radius small bob (i.e. partly inflated) with $r_0 \sim 4.0$ cm, a fixed-radius large bob (i.e. fully inflated) with $r_1 \sim 5.8$ cm, and a pulsating bob (i.e. inflating and deflating in the range $0.7r_0 < r(t) < r_1$).

Activation of the pulsating routine of the bob is enabled via a manually actuated syringe which pulls and push air out and into the elastic oscillator. During all tests where the bob is pulsated, the attempt is made to maintain an inflation/deflation frequency ω_f as close as possible to $\omega_f \sim 2\omega_n$, which guarantees onset of resonance based on [5]. An example of such a routine is presented in Fig. 3, while Fig. 4 reports the profile of radius-change variation along with the translational speed of the bob throughout one entire experiment.

The results from these first series of tests are reported in Fig. 5 and 6 respectively for the case of $\omega_n \sim 1.0$ and 2.0 Hz, where the displacement of the *larger*, *smaller* and *pulsated* bob are compared. Despite the appearance of certain localized effects which can be ascribed to the added-mass variation (see for instance the larger amplitude of the first oscillation observed in Fig. 5 in the case of the pulsated actuation), the pulsating routine is not found to trigger parametric resonance.

V. Discussion

The experiments fall within the range of Stokes number $49 < \epsilon < 63$. Also, based on the definition of Reynolds number $Re = 4\,(X/r_0)\,\epsilon^2$ (with X being the initial amplitude of oscillation), our tests lie in between $28800 < Re < 63500$. This confirms that the index of added-mass recovery $\sigma^* = \frac{4\dot{r}}{\omega_n X}\sqrt{Re}$ consistently ranges within $948 < \sigma^* < 1056$. Based on [12], these results confirm that, for the conditions tested, added-mass recovery should indeed take place, thus demonstrating that the reason for not observing the onset of parametric resonance is to be looked into experimental error.

The linear damping factor due to mechanical friction can be estimated by calculating the logarithmic decrement when the oscillator has slowed down enough to neglect the contribution from fluid drag. This provides an estimate for the damping factor due to non-fluid terms of the order of 0.01, which ensures that viscous losses from the experimental apparatus are indeed negligible.

Hence, the major issue with the experiments lies in the difficulty of actuating the inflation/deflation routine in a consistent fashion and, more importantly, in ensuring that $\dot{m}_a$ occurs somewhat in phase with $\dot{x}$. The manual activation of this parametric oscillator qualitatively resembles the capability of setting a swing into resonance by modifying its moment of inertia. This problem can either be resolved by automating the pulsation routine and implementing a control based on the velocity of translation of the bob, or enforcing lower frequency of oscillation. The attempt to perform experiments at a lower frequency was pursued here by increasing the mass m of the system. This approach, however, affects the time-scale of the response of the oscillator, thus requiring the activation to be performed longer before a visible effect is felt. Indeed, the tests performed at a higher frequency (where a lower m is used), Fig. 6, manifest an extended amplitude of oscillation during the first two oscillations of the pulsated bob, which suggest a possible contribution from added-mass variation. Once the oscillations of the bob fall below a certain amplitude, the values of ϵ and σ^* become too low in order for added-mass to practically produce any thrust. This suggests that

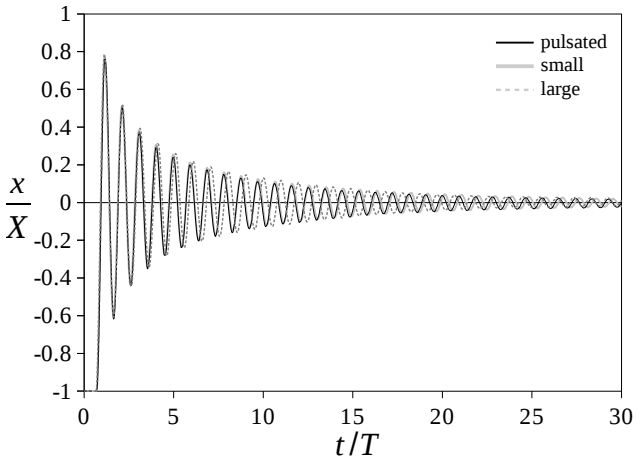

Fig. 5. Displacement of the submerged oscillator for the case of $\omega_n \sim 1.0$ Hz. The profiles *small*, *large* and *pulsated* respectively refer to the case of the partly inflated sphere, the fully inflated sphere and the case where the sphere is cyclically inflated and deflated.

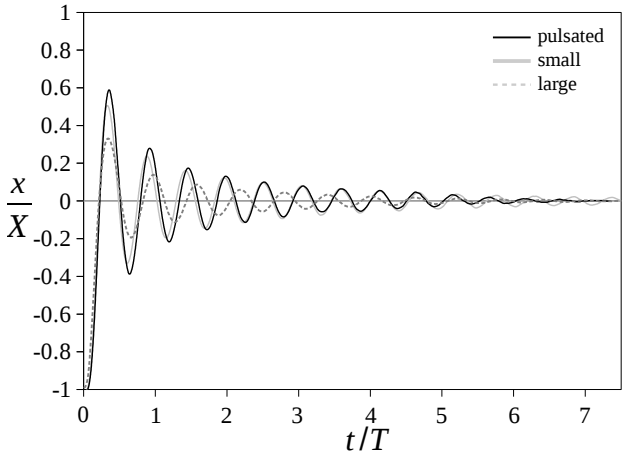

Fig. 6. Displacement of the submerged oscillator for the case of $\omega_n \sim 2.0$ Hz. The profiles *small*, *large* and *pulsated* respectively refer to the case of the partly inflated sphere, the fully inflated sphere and the case where the sphere is cyclically inflated and deflated.

effective activation of the pulsated routine must occur before the systems is damped beyond a critical threshold.

VI. Conclusion

The results presented in this article constitute the first attempt to demonstrate the role of added-mass variation on the production of thrust of submerged shape-changing bodies. Despite inconclusive, the outcome from these experiments highlight the limitation of the existing mechanical system and underscore the critical elements which require to be improved in order for added-mass recovery to become measurable. Having demonstrated that these tests fall within the range of Stokes number and σ^* values which are known to support the generation of added-mass recovery, we associate the cause for the non-occurrence of resonance to the misalignment of added-mass variation and translational velocity of the oscillator. This ensures that a revision of the actuation routine capable of ensuring the correct frequency of pulsation and correct phasing with the translation of the oscillator will yield the onset of parametric resonance.

Acknowledgment

This work was supported by the Natural Environment Research Council (grant number NE/P003966/1) and the Lloyds Register Foundation.

References

[1] G. Weymouth and M. Triantafyllou, "Ultra-fast escape of a deformable jet-propelled body," *Journal of Fluid Mechanics*, vol. 721, pp. 367–385, 2013.

[2] G. Weymouth, V. Subramaniam, and M. Triantafyllou, "Ultra-fast escape maneuver of an octopus-inspired robot," *Bioinspiration & Biomimetics*, vol. 10, pp. 1–7, 2015.

[3] W. Johnson, P. D. Soden, and E. R. Trueman, "A study in met propulsion: an analysis of the motion of the squid, *Loligo Vulgaris*," *Journal of Experimental Biology*, vol. 56, pp. 155–165, 1972.

[4] M. Krieg and K. Mohseni, "Modelling circulation, impulse and kinetic energy of starting jets with non-zero radial velocity," *Journal of Fluid Mechanics*, vol. 79, pp. 488–526, 2013.

[5] F. Giorgio-Serchi and G. D. Weymouth, "Drag cancellation by added-mass pumping," *Journal of Fluid Mechanics*, vol. 798, 2016.

[6] F. Giorgio-Serchi, A. Arienti, and C. Laschi, "Underwater soft-bodied pulsed-jet thrusters: Actuator modeling and performance profiling," *International Journal of Robotics Research*, 2016.

[7] F. Giorgio-Serchi, F. Renda, M. Calisti, and C. Laschi, "Thrust depletion at high pulsation frequencies in underactuated, soft-bodied, pulsed-jet vehicles," in *MTS/IEEE OCEANS*, Genova, Italy, May 2015.

[8] F. Renda, F. Giorgio-Serchi, F. Boyer, and L. C., "Modelling cephalopod-inspired pulsed-jet locomotion for underwater soft robots," *Bioinspiration & Biomimetics*, vol. 10, 2015.

[9] J. R. Morison, M. O'Brien, J. Johnson, and S. Schaaf, "The force exerted by surface waves on piles," *Petroleum Transactions*, vol. 189, pp. 149–154, 1950.

[10] F. Giorgio-Serchi and G. D. Weymouth, "Underwater soft robotics, the benefit of body-shape variations in aquatic propulsion," in *Soft Robotics: Trends, Applications and Challanges*, ser. Biosystems & Biorobotics. Springer, 2016, vol. 17, pp. 37–46.

[11] E. K. Lavroskii and A. M. Formal'skii, "Optimal control of the pumping and damping of a swing," *Journal of Applied Mathematics and Mechanics*, vol. 57, pp. 311–320, 1993.

[12] S. C. Steele, G. D. Weymouth, and M. S. Triantafyllou, "Added mass energy recovery of octopus-inspired shape change," *Journal of Fluid Mechanics*, vol. 810, p. 155174, 2017.